

A K BAND DEEP GALAXY SURVEY

L. L. COWIE,^{1,2} J. P. GARDNER,^{1,2} S. J. LILLY,^{1,2} AND I. MCLEAN³

Received 1990 March 6; accepted 1990 June 4

ABSTRACT

We report the results of a K band deep imaging survey, with a 5σ limit of $K = 21.4$ for galaxy detection (1σ per $1''.2$ pixel of $K = 24.2$). Number counts from $K = 16.5$ to $K = 21.25$ are given. Comparison with optical survey data on the field shows objects as red as $(I-K) = 5$ which most probably correspond to high-redshift ($z \sim 2$) normal galaxies. No evidence is seen for any population of high- z protogalaxies or brown dwarfs. The results are placed in the context of extragalactic background light measurements.

Subject headings: galaxies: general — galaxies: redshifts — infrared: sources

I. INTRODUCTION

The potential importance of near-infrared observations for deep cosmological studies has always been recognized. This is because the only way to obtain comparable samples of galaxies is to select them at a wavelength that systematically increases with redshift. An ideal combination is to use a deep infrared survey to produce samples of high-redshift objects that will complement optically selected samples at low redshift. This methodology also ties the selection band to that part of the spectrum of a galaxy in which most of the energy in normal starlight is emitted. Such a uniformly selected sample makes a number of important investigations possible. The distribution of optical–infrared color as a function of redshift can give information on the general history of star formation in the universe, including the evolution of galactic disks and the formation of S0 and elliptical galaxies. It may even be possible to constrain the luminosity-evolution/geometry combination sufficiently to place limits on the values of the deceleration parameter, q_0 , and the Hubble constant.

Hitherto, most studies of galactic evolution have been based on samples of galaxies selected at different redshifts in rather different ways, i.e., a conventional optically selected sample at high redshift is really being selected on the basis of the rest frame ultraviolet radiation. Such a bias can be especially severe when it is realized that most of the evolutionary effects being sought are manifested as changes in the galaxy continuum at these ultraviolet wavelengths. There have been attempts to study galaxies selected at different redshifts in a more homogeneous manner. For example, well-defined samples of radio galaxies at different epochs can be constructed quite easily. However, the presence of such an unusual and easily recognizable property, i.e., the strong radio emission in this case, virtually guarantees that the population of galaxies selected will not be at all representative of the population of “normal” galaxies.

In order to be of interest in the way described above, a K band survey must reach to a depth where high- z objects will be included in the sample. In rough terms and depending on the cosmology and the degree of evolution, we may expect this to occur at around $K = 20$ (Lilly and Cowie 1987). In the particu-

lar case of the high- z radio galaxies, which correspond to objects several times larger than present-day L_* galaxies, $z = 1$ corresponds to objects with $K \sim 17$ (e.g., Lilly and Longair 1984). A sample reaching beyond $K = 20$ will therefore contain a majority of high- z objects at substantial look-back times.

Because of the extreme technical difficulties only the most limited results were obtained prior to the advent of the new generation of infrared arrays (e.g., Boughn, Saulson, and Uson 1986; Collins and Joseph 1988). Even with the IR arrays, the deepest results to date are those of Elston, Rieke, and Rieke (1988) with an approximate 5σ limiting depth of galaxy detection of $K \sim 18$. At this level most objects are relatively normal low- z galaxies, though Elston, Rieke, and Rieke did find two quite red [$(I-K) \sim 3.5$] galaxies which may be unusually luminous elliptical galaxies at $z \sim 0.8$ (Elston, Rieke, and Rieke 1989).

In the present *Letter*, we shall describe the results of a survey which has used the new infrared arrays to go to a 5σ limiting depth for galaxy detection of $K = 21.4$ by using sophisticated flat-fielding techniques together with extremely long exposure times (up to 22 hr) on a 4 m telescope.

II. OBSERVATIONS

The observations described here were obtained at the 3.9 m UKIRT telescope with the IRCAM and IRCAM2 cameras that utilize SBRC InSb detectors with a 58×62 format (McLean 1987). In order to obtain a reasonable field of view $1''.2$ pixels were used throughout. The $480 e^-$ read noise and full well capacity of $975,000 e^-$ allow near sky background-limited exposures to be obtained.

Because of the brightness of the K band background (currently $12.6 \text{ mag arcsec}^{-2}$ in IRCAM from a combination of sky, telescope, and instrument) extremely accurate flat-fielding is required (around 1 part in 10^5 in each pixel) to obtain interesting cosmological depths. Fortunately, the powerful technique of median sky flat generation, when carefully tuned, allows essentially perfect flat-fielding for even very long exposures.

The median sky flat technique consists of obtaining multiple exposures, each moved by a few arcseconds in a nonreplicating pattern. The individual exposure time is optimized by making each exposure sky background-limited but otherwise as short as possible to maximize the rate of acquisition of frames while not making the overhead from telescope slewing too large a fraction of the total time. Median values of a large number of

¹ Institute for Astronomy, University of Hawaii.

² Visiting Astronomer, United Kingdom Infrared Telescope (UKIRT) which is operated by the Royal Observatory Edinburgh for the Science and Engineering Research Council.

³ Joint Astronomy Centre.

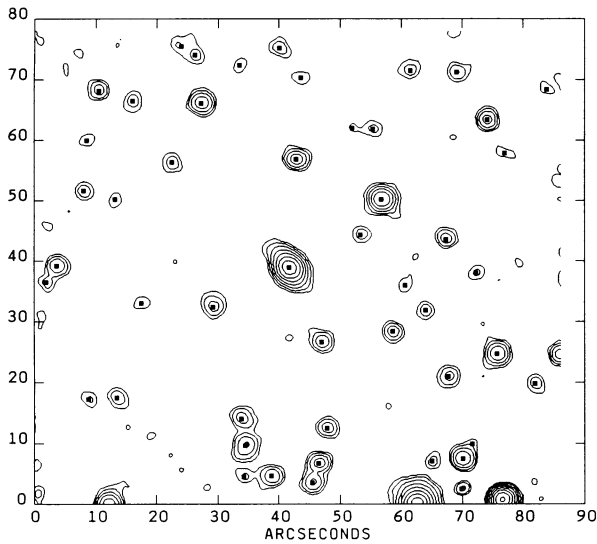


FIG. 2a

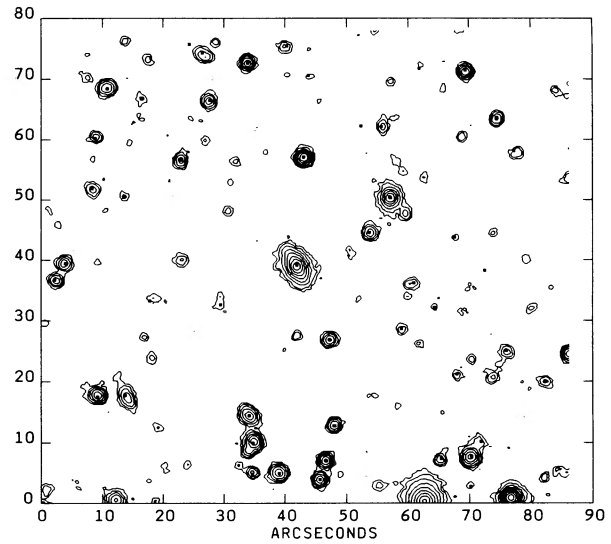


FIG. 2b

FIG. 2.—(a) K band of 22.4 hr exposure on SSA 22 field centered at $22^{\text{h}}15^{\text{m}}01^{\text{s}}.0$ and $-00^{\circ}00'09''$ (1950). Objects detected by an automated photometry program and determined to be above the 5σ level in a $3''.5$ aperture are marked with squares. Each contour rises by a factor of 2. (b) K band-detected objects (small solid squares) are shown on optical picture of the same area (a sum of exposures on the 3.6 m CFHT telescope and the University of Hawaii 88 inch [2.2 m] telescope consisting of 6.3 hr of equivalent 3.6 m time in *I*, 4.7 hr in *V*, and 4.5 hr in *B*). All but three of the $>5\sigma$ K band objects are clearly seen in the optical picture, as are many of the fainter K band objects. The FWHM on the optical exposure is $0''.8$ or roughly half that of the K band image.

exposures on either side of an individual exposure are used to generate the sky flat for the exposure, and the exposures are then registered and added to form the final frame during which cosmic rays and other defects are simply filtered out. The individual frames also provide subpixel sampling of the final image which allows us to obtain considerably higher spatial resolution than would be expected from the Nyquist criterion applied to single frames.

Extensive experimentation has shown that the currently optimal times between slews with IRCAM at UKIRT is around 80 s. Shorter times degrade on-target efficiency while longer times result in poorer flat-fielding. At 80 s, with flats generated from a median of eight frames around each individual frame, we are within 0.1 mag of the theoretical noise limit, and the flat-fielding is nearly perfect.

The current data consist of two sets of exposures. The first is a wider field coverage of 14 arcmin^2 with various limiting depths which was obtained during earlier nonoptimized observations and from the outer regions (low coverage) in deeper exposures. Throughout this area the 5σ limiting magnitude in a $5''$ diameter aperture (which contains nearly all the light) is fainter than $K = 19$. Fifty-seven objects are detected in these fields to $K = 19$ and are used in the present Letter only to define the bright end of the number counts. The colors of these objects will be described elsewhere.

The second and more fundamental data set for the present Letter is a single optimized exposure of a 1.6 arcmin^2 field with an on-target exposure time of 22.4 hr. This field was centered on the 22^{h} small selected area at R.A. = $22^{\text{h}}15^{\text{m}}00^{\text{s}}$, decl. = $00^{\circ}00'00''$ (1950), where extensive optical data in *I*, *V*, *B*, and *U* is available and where all but one of the $B < 24$ objects have been spectroscopically studied (Cowie *et al.* 1988; Lilly, Cowie, and Gardner 1990). The FWHM image quality is $1''.7$. This image is shown in Figure 1 (Plate L1) and Figure 2. The 5σ limiting magnitude in a $3''.5$ diameter aperture which contains nearly all the light even for the most extended objects is $K = 21.4$. To this limit 49 objects are detected in this field of

which all but three are seen in an ultradeep optical image (16 hr of exposure on a 3.6 m telescope) shown in Figure 1 and Figure 2b.

These data in conjunction with the wide field sample allow us to determine the K band number counts that are shown in Figure 3. At the faintest end shown, the counts require a correction for a small amount of object overlap owing to the relatively poor image quality. This was determined empirically by adding objects of known magnitude to the images and then attempting to retrieve them. The counts have not been

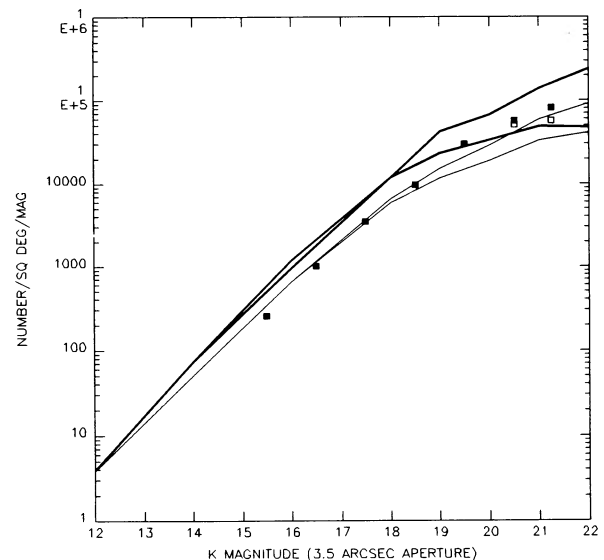


FIG. 3.—The raw K band number counts (open squares) and corrected number counts (solid squares) compared with the models of Yoshii and Takahara. The thin lines show predictions for non evolving galaxies (lower curve, $q_0 = 0.5$; upper curve, $q_0 = 0.02$) and the thick lines for evolving galaxies (lower curve at faint end, $q_0 = 0.5$; upper curve, $q_0 = 0$):

PLATE L1

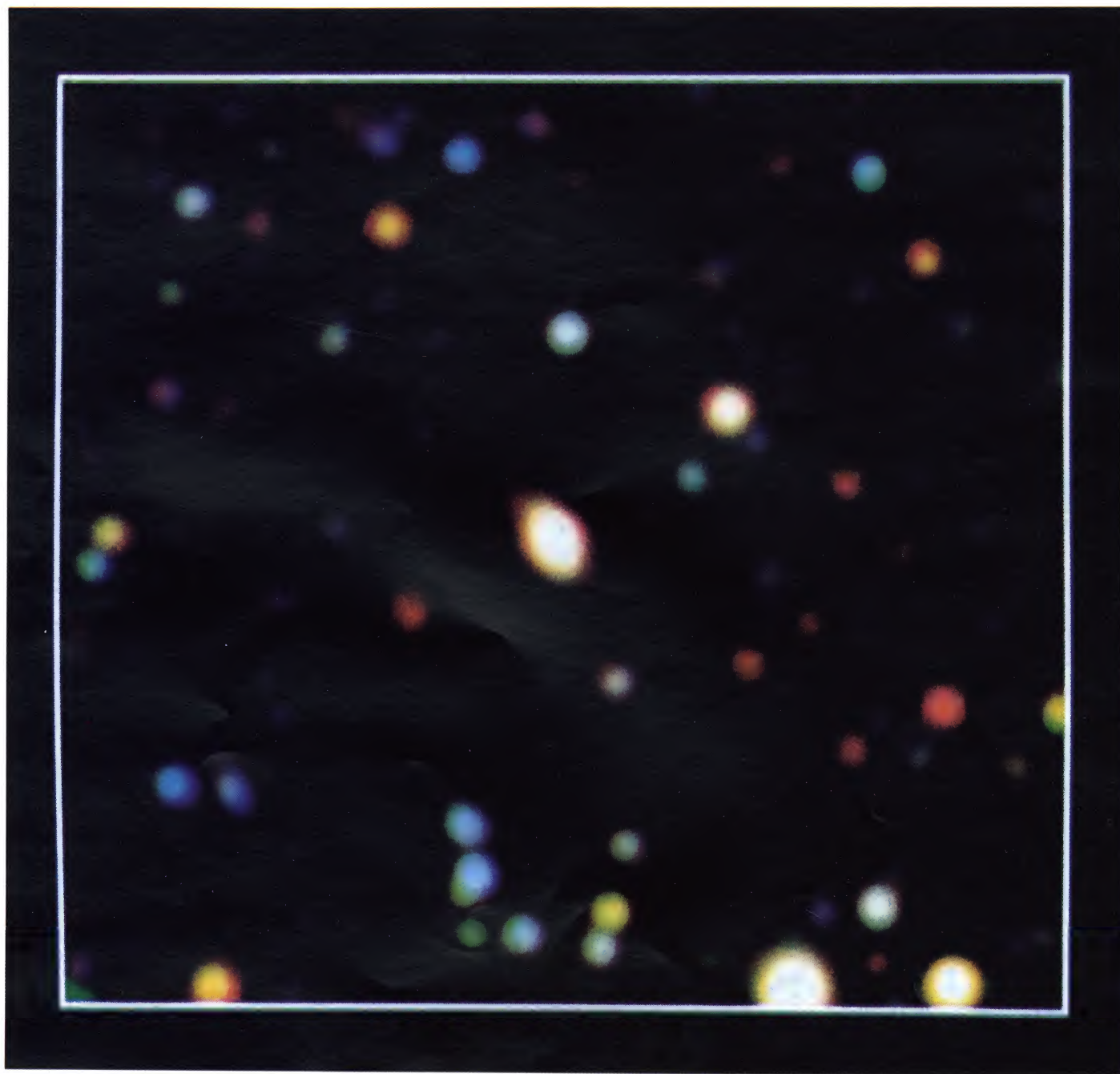


FIG. 1.—A multicolor photographic representation of the deep field where red corresponds to the K band image, green to the I , and blue to $(B + V)$. The data have been smoothed to a $1''.8$ FWHM and the color balance set such that an I_m galaxy would appear white. A few of the brightest objects are saturated in the color balance and appear whitish when they are much redder.

COWIE *et al.* (see 360, L2)

extended beyond the point at which this correction becomes at all significant.

Also shown for comparison are Yoshii and Takahara's (1988) model predictions for unevolving (*thin lines*) and evolving galaxies (*thick lines*). To $K = 21.25$, the counts agree reasonably well with a nonevolving $q_0 = 0$ model though the slope is slightly steeper. However, at the faint end, they are slightly more than a factor of 2 higher than predicted by a $q_0 = 0.5$ nonevolving model and about a factor of 2 lower than expected in a $q_0 = 0$ model with evolution. The shape of the counts does not agree well with the $q_0 = 0.5$ models irrespective of the degree of evolution. However, given our relatively poor understanding of the evolution together with the possibility that there may have been significant merging in the higher z objects which constitute the bulk of the faint end population, it would be improper to draw any cosmological conclusion from these data.

Of more interest are the colors of the detected objects and a $(B-I)$ versus $(I-K)$ color-color diagram for the K band sample is shown in Figure 4 together with star tracks and simple non-evolved galaxy models as a function of z . Because low-redshift galaxies have similar $[(I-K)_{AB} \sim 0]$ IR colors, $I-K$ is primarily a redshift diagnostic. This can be seen in Figure 4, where objects at larger redshifts have progressively redder $(I-K)$ colors as the ultraviolet portion of the galaxy spectrum shifts into the I window. $(B-I)$ on the other hand primarily provides a diagnostic of galaxy morphology. Finally, it should be noted that the star-tracks are clearly separated.

On Figure 4 objects which are found to have stellar profiles on a deep high-resolution V band image of the field ($\text{FWHM} = 0''.6$) are shown as stars. Most of these follow the star track although there is also clearly a very small number of unresolved galaxies. The combination of morphology and colors suggest that six of the 49 objects are stars. The field is at Galactic latitude -44° so that this would translate to a cumulative polar star density of 9000 per square degree to $K = 21.4$. All but one of the stars are M type. Within the small number uncertainties, this cumulative count is completely consistent with model expectations (Bahcall and Soneira 1981; Lilly and Cowie 1987).

At the brighter end ($K < 19$), all but one of the galaxies have colors consistent with their being low-redshift galaxies. Many of these have spectroscopic identifications (Lilly, Cowie, and Gardner 1990) that agree well with the redshift and type that would be inferred from Figure 4. However, even at this magni-

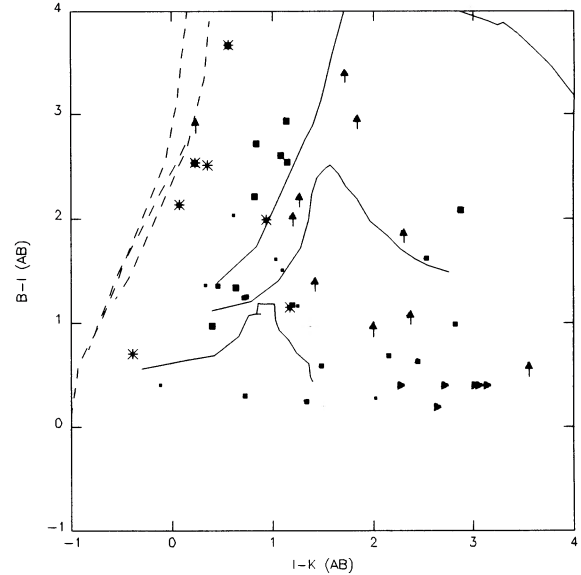


FIG. 4.— $B-I$ versus $I-K$ for 5σ selected objects in the deep K band field. The plot is given in AB magnitudes [$I-K(AB) = I-K - 1.5$, $B-I(AB) = B-I - 0.6$] so that flat f_{nu} objects lie at $(0, 0)$. The size of the squares represent the K magnitude, and lower bounds are shown at the 2σ level for objects not detected in B (upward arrows) or I (right-pointing triangles). Compact objects are marked as asterisks. The dashed lines show the positions of stars on the color-color plot and the solid lines Im , Sbc , and E galaxies [blue to red in $(B-I)$] at redshifts from 0 to 2 [blue to red in $(I-K)$].

tude, one object (SSA 22-19) has an extremely red color with $(I-K)$ of 4.4 and $K = 18.6$ and its SED is similar to a $z \sim 2$ spiral galaxy (Fig. 5). This object lies at $(77'', 25'')$ in Figure 2.

As one moves to fainter magnitudes the fraction of very red $(I-K)$ galaxies increases until a majority are at the redder colors at $K > 20$. The object with the reddest well-defined color (SSA 22-58) has $(I-K) = 5.1 \pm 0.5$ at a K magnitude of 19.8. (This object is at $[68'', 43'']$.)

As might be expected from the consistency of the number counts and the models, the number of moderate-redshift ($z \sim 2$) galaxies inferred from Figure 4 is very similar to simple model expectations that are relatively certain because of the small amount of evolution in the rest frame wavelength corresponding to the K band. Of more interest is the high number of redder (spiral-like) objects that can be placed at these z values (more than a dozen) versus the much smaller number (three) of

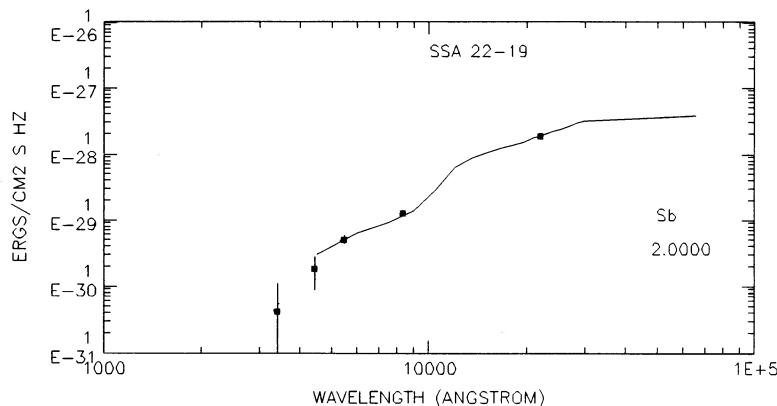


FIG. 5.—Spectral energy distribution of the brightest red object (SSA 22-19) in the K band sample. The solid line shows the SED of an unevolved spiral galaxy at $z = 2$.

blue (I_m -like) objects. These latter objects are the flat spectrum galaxies in this field described by Cowie *et al.* 1988). It appears at least possible based on Figure 4 that the distribution of galaxy colors at $z \sim 2$ is not substantially different from that seen locally, and that the bulk of galaxies at such redshifts are red, not blue.

III. DISCUSSION

The reddest objects in the present sample are about half a magnitude redder than the $z = 3.395$ radio galaxy 0902 + 34 which has $(I - K) = 4.5$ (Lilly 1988, 1990) and about 1.5 mag redder than the Elston, Rieke, and Rieke (1988) objects. They are also redder even than extreme M stars and brown dwarf candidates such as LHS 2924 ($I - K = 4.6$) or Gl 569B ($I - K = 4.3$) (Probst and Liebert 1983; Forrest, Skrutskie, and Shure 1988), so that they cannot be formed from a stellar population at low redshift.

The colors are most easily understood if these are indeed the high-redshift galaxies expected at these magnitudes. As discussed above, the spectral energy distributions of some of the reddest objects, shown in Figure 4, can be fitted by spiral galaxy SEDs redshifted to $z \sim 2$. The SED fits do not necessarily mean that these are $z = 2$ unevolved spiral galaxies but do show that the ultrared galaxies can be understood as high- z galaxies. Even for a completely unevolved elliptical galaxy ($I - K$) does not reach the values of the reddest objects until $z > 1$ (Fig. 4), and any evolutionary processes might be expected to render the galaxy bluer and hence force us to place it at higher redshift. If the reddest galaxies are placed at $z \sim 2$, their observed $M_K = -26 \rightarrow -27$ depending on q_0 . Allowing for only passive evolution of about 2 mag (Lilly and Longair 1984) to this redshift, this would correspond to a current $M_V \sim -21.5 \rightarrow -22.5$ or a galaxy which is just brighter than L_* . Any amount of luminosity evolution beyond the passive correction would make these galaxies correspond to sub- L_* objects at the present time.

We might have hoped to see evidence for galaxy progenitors since the K band is sensitive to such objects out to large distances ($z \sim 20$). In particular, a massive galaxy forming $2 \times 10^9 M_\odot$ of metals, over the local Hubble time at a given redshift, should have a K magnitude brighter than 22 in a closed universe (Cowie 1988). Such objects at $z > 4$ should be seen in K

and perhaps I , but not at wavelengths of V or shorter. The average sky surface brightness of such a protogalaxy population is approximately in the range 17–20 K mag arcmin $^{-2}$ (Songaila, Cowie, and Lilly 1990) so that the number density should be 10–100 $\{K/22\}^{-1}$ arcmin $^{-2}$. However, we see no compelling evidence for the presence of any such objects in either the wide or the deep data. Of the 43 galaxies in the deep field, all but three are detected in I and all but five in $(B + V)$. The small number of undetected objects are all at the faint end of the K band sample, and their colors are quite consistent with being similar to brighter objects in the field which we detected optically.

The progenitors could be missed if $q_0 = 0$, when they could be fainter, or if they are in smaller pieces at time of formation, or if substantial amounts of dust were present in the galaxies or in the intergalactic medium. Deeper studies to reach at least 1 mag fainter appear technically possible and may reach the progenitor objects even in the $q_0 = 0$ case.

We also see no evidence of ultrared stars (Fig. 4) which might correspond to a field population of brown dwarfs. However, the field of view is sufficiently small that even optimistic predictions would only give a fraction of a source/field (Lilly and Cowie 1987).

Another approach which may be of considerable interest is to search for “missing light” by comparing observed backgrounds of known objects in the near IR with measurement of the near-IR diffuse light such as will be obtained with *COBE*. The observed sky brightness in the K band sample is shown in Figure 6, together with present upper limits on the diffuse light including the possible near-IR background suggested by Matsumoto, Akiba, and Murakami (1988). The contribution of objects seen in K but not B is also shown on the figure and is only a small fraction of the sky light as would be expected from a high- z nonevolved galaxy population. Finally the cross-hatched region shows the surface brightness expected from the ultraviolet rest frame region of a forming galaxy population (Songaila, Cowie, and Lilly 1990). If the *COBE* results confirm the data of Matsumoto *et al.*, then there must be a new population containing a large amount of light, but comprised of very faint objects. If on the other hand the *COBE* results closely approach the observed galaxy background, we may be able to measure the amount of excess light present which could be attributed to a possible protogalaxy population.

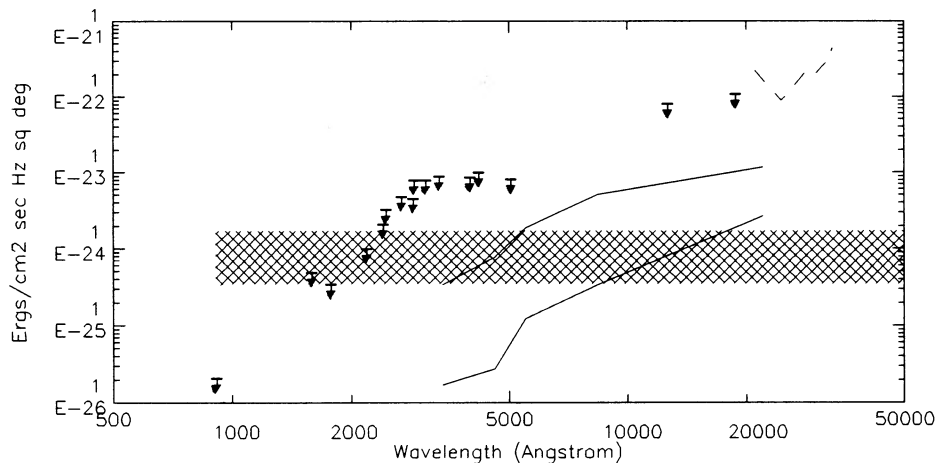


FIG. 6.—The background light from the total K band sample (upper line) and from the reddest objects (detected in K but not in B) lower thin line are compared with upper limits on the extragalactic background light and also the surface brightness expected at rest wavelengths $\lambda < 4000 \text{ \AA}$ for the population of forming galaxies (Songaila *et al.* 1990). The IR background suggested by the observations of Matsumoto *et al.* is shown as a dashed line.

We would like to thank the staff of UKIRT, and in particular Dolores Walther, for their outstanding support in obtaining the K band data. The optical data described were obtained using the Canada-France-Hawaii Telescope and the Uni-

versity of Hawaii's 88 inch telescope, and we thank both organizations for their support. This research was supported primarily by the State of Hawaii, but also by NSF 87-18275 and by NASA grant NAGW 959.

REFERENCES

- Bahcall, J. N., and Soneira, R. M. 1981, *Ap. J. Suppl.*, **47**, 357.
 Boughn, S. P., Saulson, P. R., and Uson, J. M. 1986, *Ap. J.*, **301**, 17.
 Collins, C. A., and Joseph, R. D. 1988, *M.N.R.A.S.*, **235**, 209.
 Cowie, L. L. 1988, in *The Post Recombination Universe*, ed. N. Kaiser and A. Lasenby (NATO Advanced Science Series), p. 1.
 Cowie, L. L., Lilly, S. J., Gardner, J. P., and McLean, I. 1988, *Ap. J. (Letters)*, **332**, L29.
 Elston, R., Rieke, M., and Rieke, G. 1988, *Ap. J. (Letters)*, **351**, L77.
 ———. 1989, *Ap. J.*, **341**, 80.
 Forrest, W. J., Skrutskie, M. F., and Shure, M. 1988, *Ap. J. (Letters)*, **330**, L119.
 Lilly, S. J. 1988, *Ap. J.*, **333**, 161.
 ———. 1990, in *The Evolution of the Universe of Galaxies: The Edwin Hubble Centennial Symposium (A.S.P. Conf. Ser., 10)*, in press.
 Lilly, S. J., and Cowie, L. L. 1987, in *Infrared Astronomy with Arrays*, ed. C. G. Wynn-Williams and E. E. Becklin (University of Hawaii Institute for Astronomy), p. 473.
 Lilly, S. J., Cowie, L. L., and Gardner, J. P. 1990, in preparation.
 Lilly, S. J., and Longair, M. S. 1984, *M.N.R.A.S.*, **211**, 833.
 Matsumoto, T., Akiba, M., and Murakami, H. 1988, *Ap. J.*, **332**, 575.
 McLean, I. 1987, *IRCAM Manual*.
 Probst, R., and Liebert, J. 1983, *Ap. J.*, **274**, 245.
 Songaila, A., Cowie, L. L., and Lilly, S. J. 1990, *Ap. J.*, **348**, 371.
 Yoshii, Y., and Takahara, F. 1988, *Ap. J.*, **326**, 1.

L. L. COWIE, J. P. GARDNER, and S. J. LILLY: Institute for Astronomy, 2680 Woodlawn Avenue, Honolulu, HI 96822

I. MCLEAN: Joint Astronomy Centre, 655 Komohana Street, Hilo, HI 96720